Author/s:
Xu, Z;Song, W;Crozier, KB

Title:
Optical Trapping of Nanoparticles Using All-Silicon Nanoantennas

Date:
2018-12-01

Citation:
Xu, Z., Song, W. & Crozier, K. B. (2018). Optical Trapping of Nanoparticles Using All-Silicon Nanoantennas. ACS PHOTONICS, 5 (12), pp.4993-5001. https://doi.org/10.1021/acsphotonics.8b01250.

Persistent Link:
https://hdl.handle.net/11343/240518

Supporting Information

Optical Trapping of Nanoparticles Using All-Silicon Nanoantennas

Zhe Xu,[†] *Wuzhou Song,*[†,‡] *and Kenneth B. Crozier**[*,†,§]

[†]School of Physics, University of Melbourne, Victoria 3010, Australia

[‡]School of Materials Science and Engineering, Huazhong University of Science and Technology, Wuhan 430074, China

[§]Department of Electrical and Electronic Engineering, University of Melbourne, Victoria 3010, Australia

Corresponding Author

*E-mail: kcrozier@unimelb.edu.au.

Methods

Device fabrication and chamber preparation. The Si nanoantennas studied in this paper are fabricated by standard electron beam lithography (EBL) and inductively coupled plasma reactive ion etching (ICP-RIE) on an Si wafer (Virginia Semiconductor Inc.). The resist used is ZEP520 (Zeon Chemicals). After etching, residual resist is removed, resulting in silicon nanoantenna arrays.

The microfluidic chamber (4 mm × 16 mm) is formed from photoresist on a 150 μm thick microscope glass coverslip as follows. The glass coverslip is first sonicated in water, baked on a hot plate to dry it, and cleaned in an oxygen plasma to remove particles etc. from the surface. This is followed by photoresist (AZ9260) coating, photolithography and development. The photoresist thickness is determined by the rotation speed of spin coater and measured with an optical profilometer. The photoresist is applied onto the cleaned coverslip while it is spinning at 500 rpm for 10 s to allow it to spread. The coverslip is then spun at 1000 rpm for 60 s, thereby resulting in a photoresist thickness of ~ 15 μm. Holes are drilled in the Si chip containing the nanoantennas to allow tubing to be added later. The Si chip is washed with acetone and rinsed with isopropanol and distilled water. It is then glued to the glass coverslip containing the microfluidic chamber with UV-cured optical adhesive, resulting in the chamber being closed. Polyethylene tubing to the Si chip is used to deliver fluid into the channel.

Trapping experiments. The experimental setup is based on an inverted optical microscope (Nikon TE2000). The optical trapping process is monitored by observing the nanosphere fluorescence after a set of filters (dichroic mirrors and shortpass filters) with an electron multiplying camera (EM-CCD, ProEM-HS: 512×512, Princeton Instruments) operated at 30 fps with an exposure time of ~ 30 ms. An optical beam shutter is used to switch on and off the light

from the continuous wave trapping laser (Laser Quantum Ventus 1064). A half-wave plate (λ_0 = 1064 nm) is used to rotate the polarization of the trapping laser beam. The *x*-polarized trapping beam is collimated and then focused by an oil immersion objective (Nikon Plan Fluorite Oil Immersion Objective, 100×, NA = 1.3) into a ~ 15 μm thick perfusion chamber (4 mm × 16 mm). The sample is mounted upside-down and aligned using a piezoelectric stage with a subnanometer position resolution. The focal spot diameter is ~ 1.2 μm. A loosely focused green laser (532 nm) is projected along the same optical path to excite fluorescence. The intensity at the sample due to the green laser is approximately five orders of magnitude smaller than that of the trapping beam. We thus expect that the contributions of the green laser to local heating and optical forces are negligible. The polystyrene nanospheres (FluoSpheres, 20 nm or 100 nm diameter, carboxylate-modified, Life Technologies) are suspended in distilled water with a trace amount of Tween 20 surfactant added, and the diluted suspension is ultrasonicated using a bath sonicator and further passed through a filter to remove aggregates, etc. The nanospheres have a coefficient of variation of about 20% for 20 nm and 5% for 100 nm respectively, according to the manufacturer (Life Technologies). The transmission of oil objective to the focal plane at 1064 nm is ~ 55%. Before the experiments, the mixture of water with Tween 20 is flowed through the channel to prevent nonspecific binding. Each experiment is done with freshly made suspension. Each pixel on the EM-CCD sensor array is 16 μm × 16 μm, which translates to around 160 nm × 160 nm in the focal plane with the 100× magnification objective.

Numerical calculations. Three-dimensional simulations are performed by the finite element method (FEM) using COMSOL Multiphysics. We use the "Wave Optics Module" to solve the near field distribution and for force determination. We begin by finding the background field ($|E_b|$) between substrate (Si or glass) and water space. We then perform a scattered field

simulation with the nanoantenna (Si or Au) being the scatterer. We use perfectly matched layers (PMLs) at the boundaries of the simulation space. To calculate the optical force with the MST, the nanoantenna and a single NS are introduced as two scatterers in the simulation. The optical trapping force on the NS is obtained by integrating the MST over its surface. The trapping energy is determined from the force map using the PDE module (partial differential equation) by solving the following equation: $-\nabla U = \vec{F}$. The refractive indices of water, glass and polystyrene are taken as 1.33, 1.45 and 1.6 respectively. The optical constant of Si is taken from Palik[1] and the optical constant of Au is taken from the data of Johnson and Christy.[2]

We use the heat transfer and laminar flow modules to solve the temperature rise distribution and fluid dynamics problems (here for steady state). This is performed as follows. The absorbed power in the Si cylinder dimer, in the Si ring, and in a region of the underlying Si substrate that has dimensions 2 μm × 2 μm × 1 μm (along *x*, *y*, *z* axes) is found from the electromagnetic simulations described above. This absorbed power is then taken as heat source power in the subsequent temperature rise distribution calculation. The heat source power is assumed to be evenly distributed, i.e., has the same density, over the Si cylinder dimer, over the Si ring and over the underlying region of the substrate (2 μm × 2 μm × 1 μm). While additional optical power is absorbed deeper into the substrate (i.e., beyond 1 μm), this absorbed power has an effect upon the temperature rise at the surface that decreases with distance. In the simulation, as shown in Figure S5, the outer boundaries and initial temperature are set to be 293.15 K. No-slip boundary conditions are employed at the boundaries between water and solids. The thermal parameters of silicon, gold, glass and water are all taken from COMSOL material library.

Figures and captions

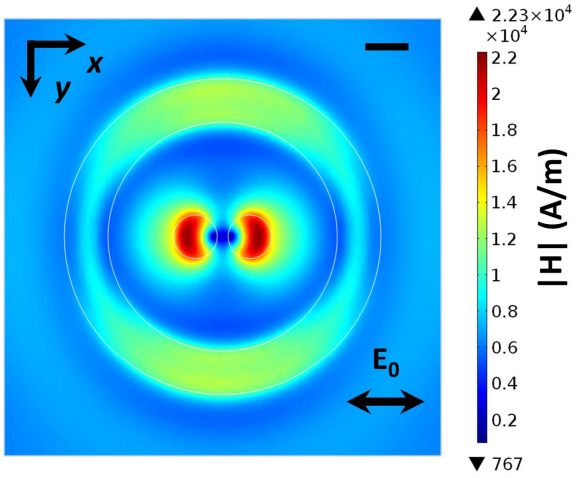

Figure S1 | Magnetic fields distribution. Plotted in the center plane of our Si nanoantenna with plane wave illumination (*x*-polarized, λ = 1064 nm, I_0 = 5 mW/μm^2). Scale bar: 200 nm.

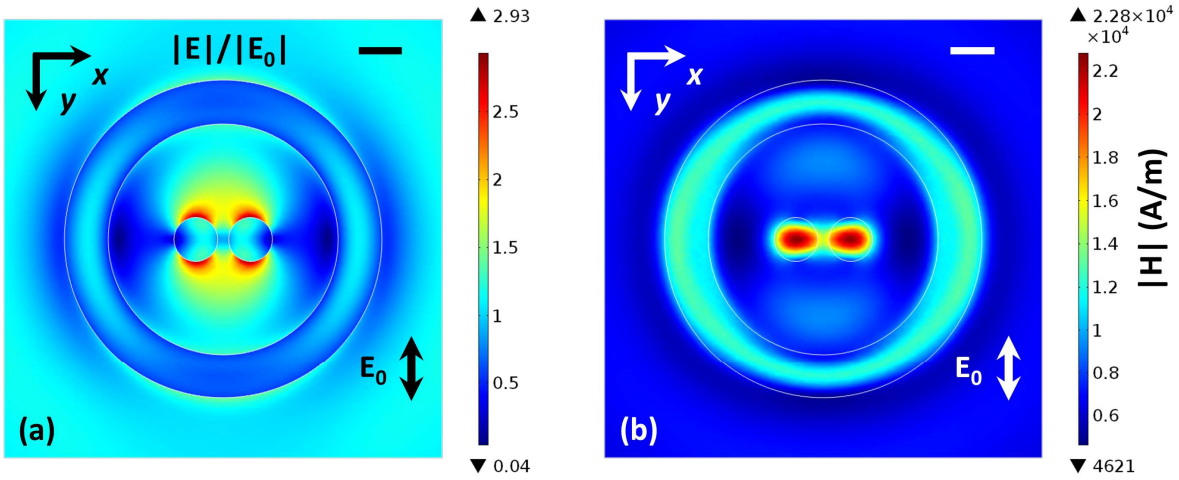

Figure S2 | Near fields for *y*-polarized illumination. (a) Electric field enhancement and (b) magnetic field amplitude in the center plane of our Si nanoantenna, for plane wave illumination (*y*-polarized, $\lambda = 1064$ nm, $I_0 = 5$ mW/μm^2). Scale bar: 200 nm.

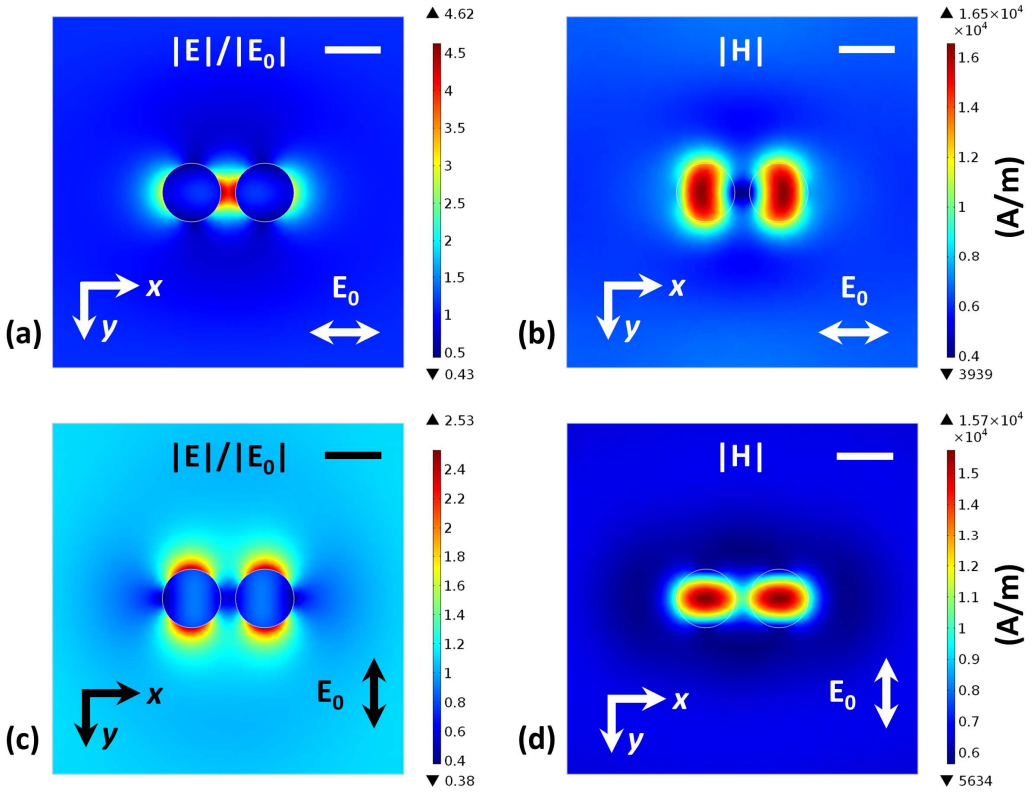

Figure S3 | Near fields in Si nanodimer. Si cylinder dimer nanoantenna (two cylinders of diameters and heights of 200 nm, 50 nm gap in between) on an Si substrate, covered with water. Plotted in the center plane ($z = -100$ nm cross section), illuminated by plane waves with different polarizations (λ = 1064 nm, I_0 = 5 mW/μm^2). (a)(b) *x*-polarized; (c)(d) *y*-polarized. Scale bar: 200 nm.

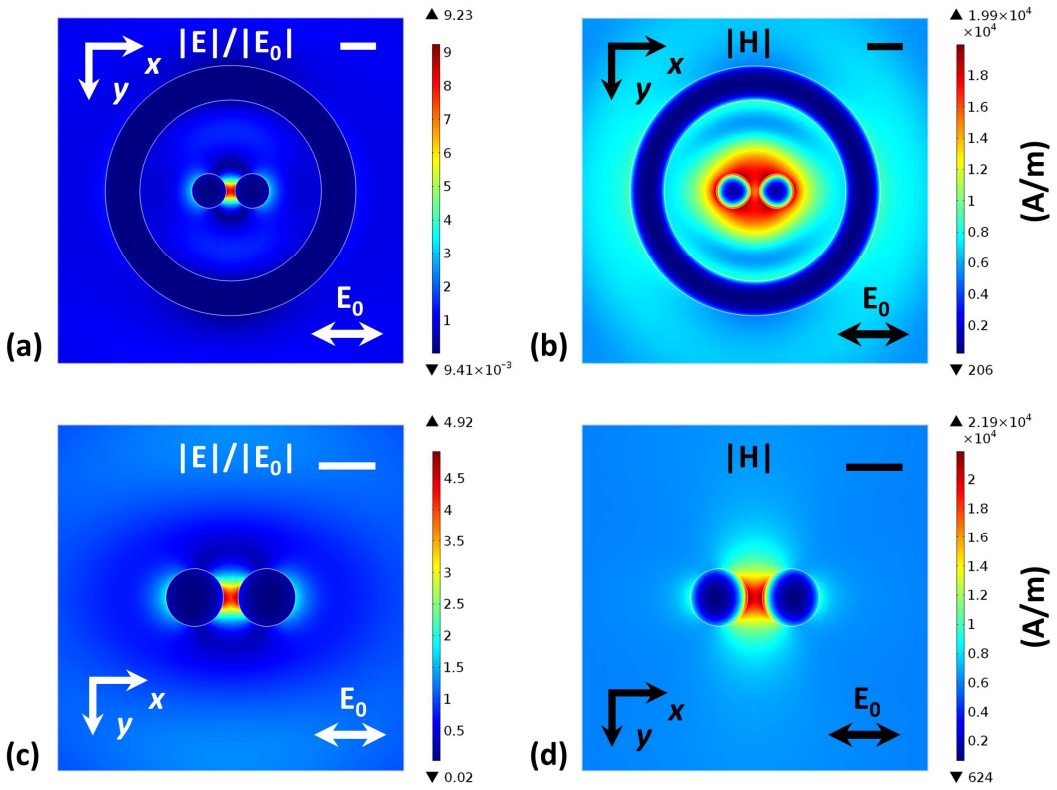

Figure S4 | Near fields in Au nanostructures. (a)(b) Au nanoantenna with same dimensions as Si nanoantenna on a glass substrate; (c)(d) Au nanodimer (two cylinders of diameters and heights of 200 nm, 50 nm gap in between) on a glass substrate, covered with water. (a)(c) Electric field enhancement, and (b)(d) magnetic field amplitude, plotted in the center plane and illuminated by plane wave with *x*-polarization (λ = 1064 nm, I_0 = 5 mW/μm^2). Scale bar: 200 nm.

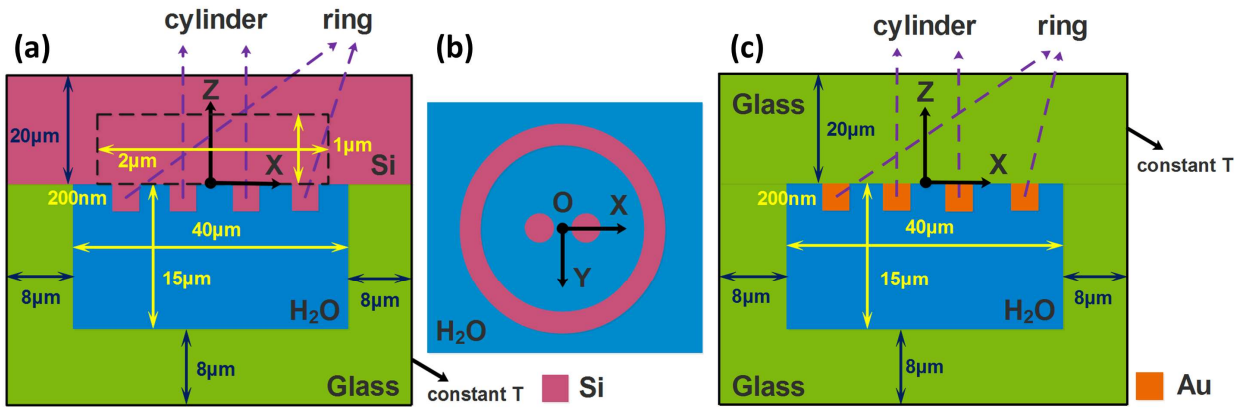

Figure S5 | Geometric configuration for heat calculation. Sketch is not to scale. (a)(b) Si nanoantenna on an Si substrate. (c) Au nanoantenna with same dimensions on a glass substrate. Black line indicates chamber boundaries at which T_0 = 293.15 K. Black dashed line in panel a indicates underlying Si substrate heat source. Si cylinders and Si ring also act as heat sources.

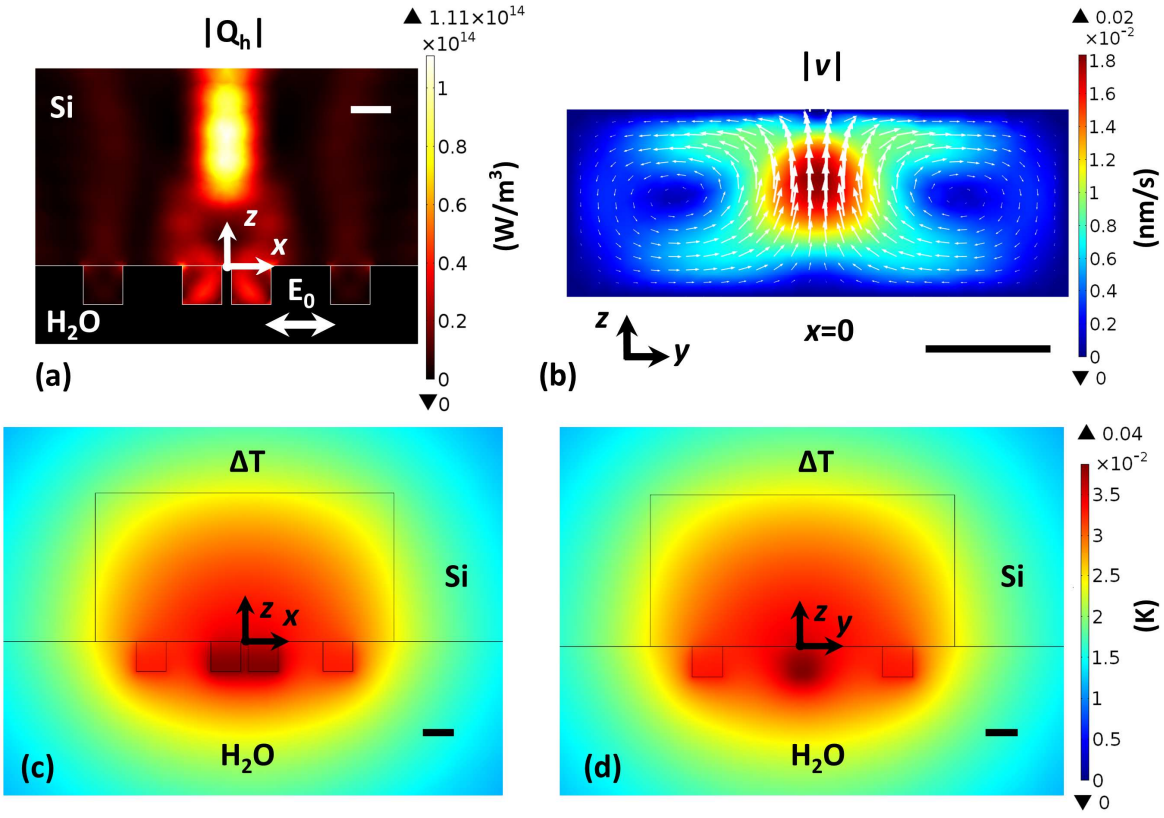

Figure S6 | Photothermal effects in Si nanoantenna. (a) Heat power dissipation density in the *xz*-plane. Scale bar: 200 nm. (b) Water convection velocity field in the *yz*-plane, plotted in both magnitude (color map: nm/s) and direction (white arrows, magnitude proportionally scaled). Chamber height is 15 μm. Scale bar: 10 μm. Steady state temperature increase profile in the (c) *xz*- and (d) *yz*-plane. Scale bar: 200 nm. White & black dots indicate coordinate system origin. I_0 = 5 mW/μm^2.

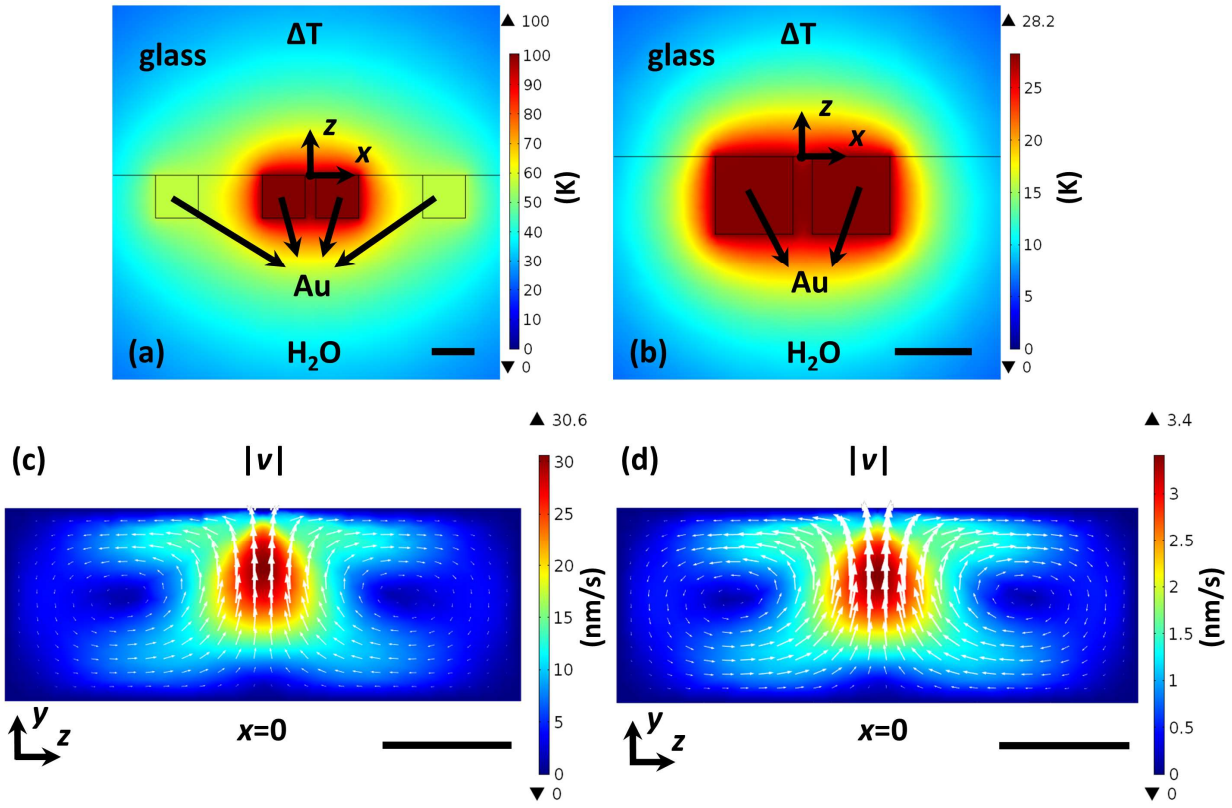

Figure S7 | Photothermal effects in Au nanostructures. (a)(c) Au nanoantenna with same dimensions as Si nanoantenna on a glass substrate; (b)(d) Au nanodimer (two cylinders of diameters and heights of 200 nm, 50 nm gap in between) on a glass substrate. (a)(b) Steady state temperature increase profile in the *xz*-plane. Black dot indicates coordinate system origin. Scale bar: 200 nm. (c)(d) Simulation of water convection velocity field in the *yz*-plane, plotted in both magnitude (color map: nm/s) and direction (white arrows, magnitude proportionally scaled). Chamber height is 15 μm. Scale bar: 10 μm. I_0 = 5 mW/μm^2.

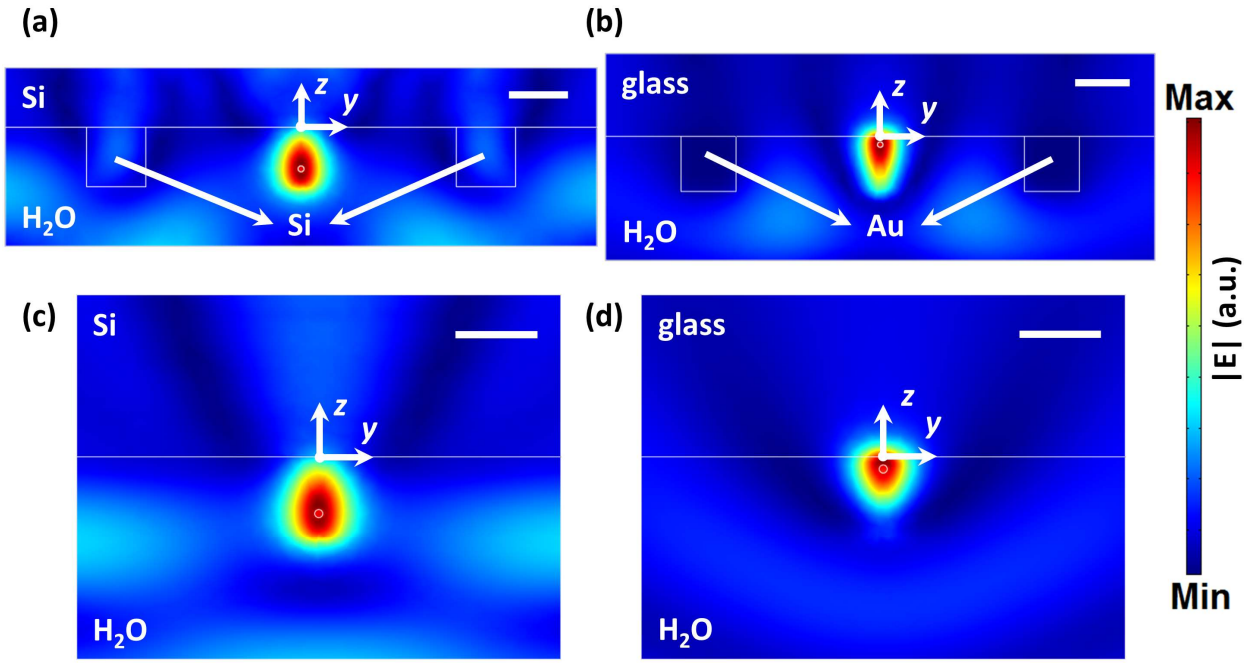

Figure S8 | Electric fields distributions, with a single NS included in simulation. Polystyrene NS: n_{NS} = 1.6, d = 20 nm. (a) Si nanoantenna on an Si substrate; (b) Au nanoantenna with same dimensions on a glass substrate; (c) Si cylinder dimer nanoantenna on an Si substrate; (d) Au cylinder dimer nanoantenna on a glass substrate. For each of these, water superstrate is used. Plane wave illumination from water side is employed (traveling in $+z$ direction, x-polarized, λ = 1064 nm). White dot indicates coordinate system origin. Center z-coordinates of NS are as follows ((x_{center}, y_{center}) = (0, 0)). (a)(c) z_{center} = −140 nm; (b)(d) z_{center} = −30 nm. I_0 = 9.5 mW/μm^2. Scale bar: 200 nm.

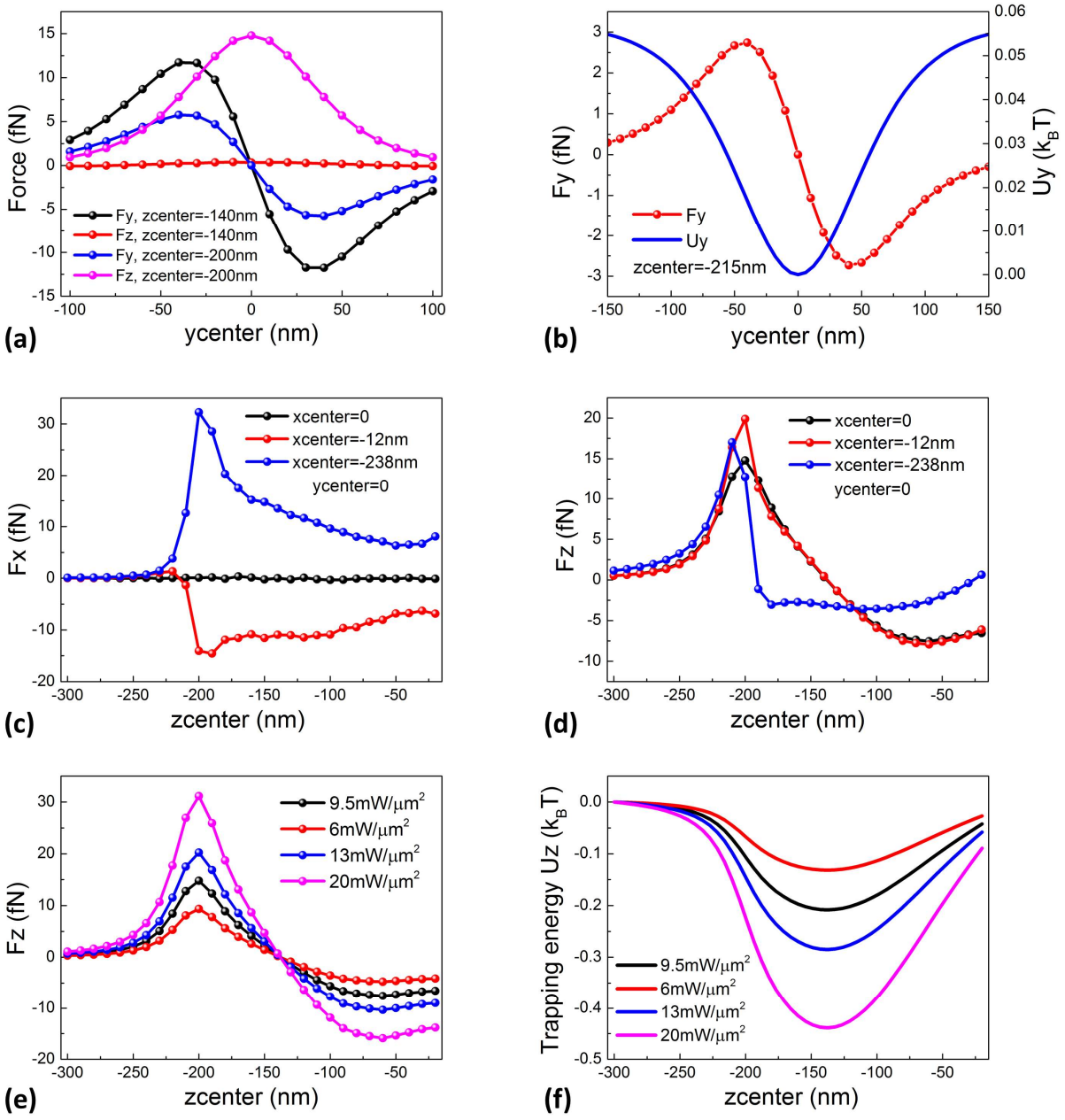

Figure S9 | MST optical forces in Si nanoantenna. Polystyrene NS: n_{NS} = 1.6, d = 20 nm. (a) F_y and F_z along y-direction (x_{center} = 0) for moving in the middle (z_{center} = −140 nm) and the edge (z_{center} = −200 nm). (b) F_y and U_y vs. NS position at 15 nm outside of nanoantenna along y-axis (x_{center} = 0, z_{center} = −215 nm). (c)(d) NS moving in the xz-plane (y_{center} = 0) along z-direction in the middle (x_{center} = 0) and around left cylinder (x_{center} = −12 nm and −238 nm, that is, 3 nm distance to Si surface) of (c) F_x and (d) F_z. (a)–(d) I_0 = 9.5 mW/μm^2. (e) Vertical force F_z and (f) trapping potential energy U_z along z-axis as functions of trapping laser intensity and position over the gap (x_{center} = y_{center} = 0). In panels b and f, $1k_BT = 4.05\times10^{-21}$ J.

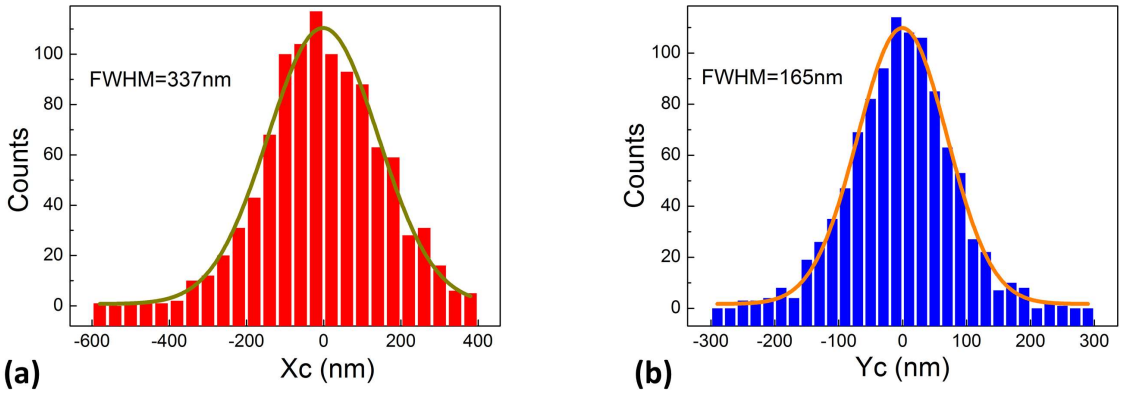

Figure S10 | Brownian motion histogram. Position histograms (1000 EM-CCD frames) of a trapped 20 nm NS, relative to trap center along *x*- and *y*-axes. Illumination intensity is I_0 = 9.5 mW/μm^2. These plots are extracted from data of Figure 4e.

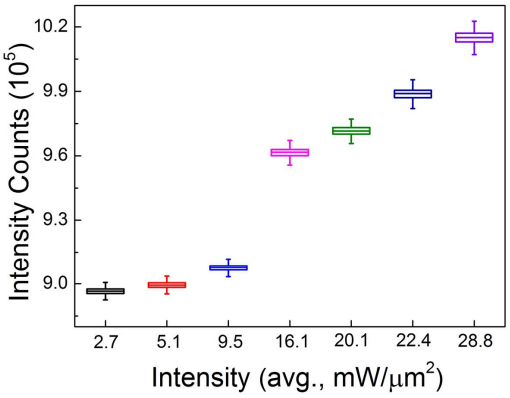

Figure S11 | Fluorescence measurement. Recorded EM-CCD intensity counts vs. trapping laser intensity (single 20 nm NSs, same green laser power, 30×30 pixel cross section, 1000 frames). Box plot measured for single trapped NSs. Background has not been subtracted from data in this plot. For each box, the center is the median, the edges of the box are the 25th and 75th percentiles, and the whiskers are the 5th and 95th percentiles.

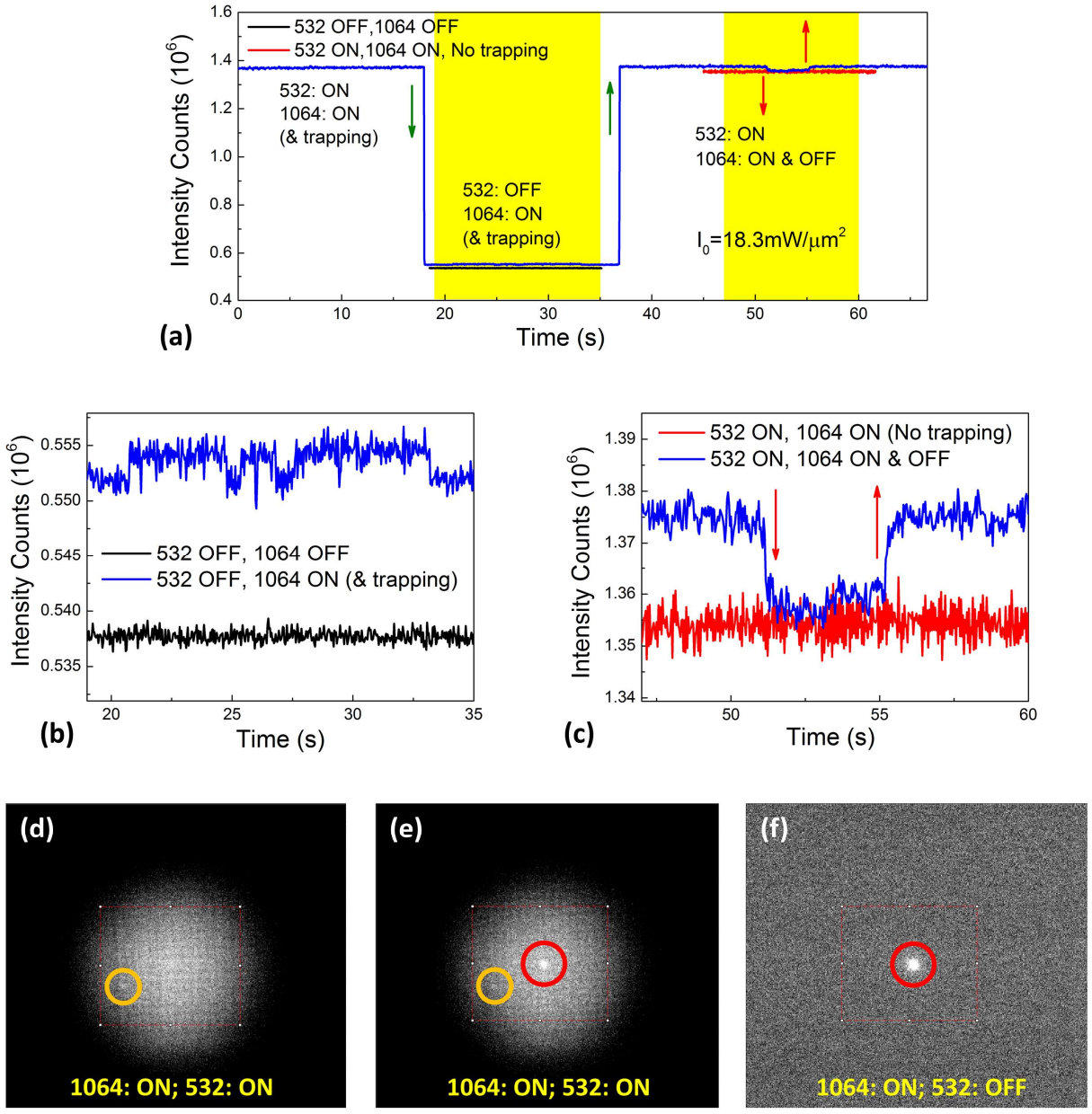

Figure S12 | Two-photon excitation. (a) Experimental fluorescence time trace indicating optical trapping, release and two-photon excitation of a single 20 nm NS (30×30 pixel cross section, I_0 = 18.3 mW/μm^2). Black and red curves, obtained in separate measurements, are included on this plot for comparison of signal levels (intensity counts). Zoom-in of panel a from (b) 19−35 s and (c) 47−60 s. (d)−(f) EM-CCD images of fluorescence. Orange circles indicate the NS that is attached to the Si surface, and the red circles indicate the NS being trapped. Switching the trapping laser off releases NS from the nanoantenna. After switching the green laser off, one observes the two-photon absorption induced fluorescence from trapped NS, but no one-photon induced fluorescence from the NS attached to the surface. Images are captured with auto-scale contrast of EM-CCD camera.

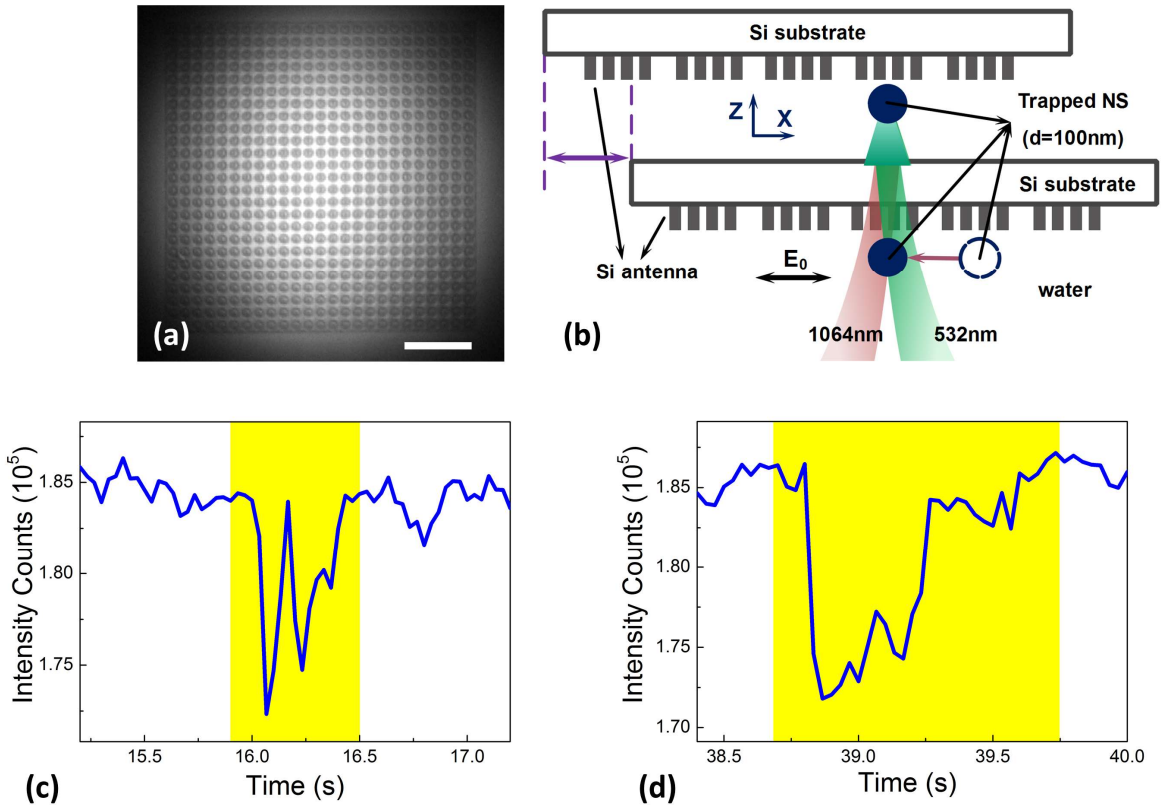

Figure S13 | Optical transport of NSs. (a) Microscope image of Si nanoantenna array chip immersed in water. Scale bar: 10 μm. (b) Schematic of trapping and transport of single NSs (d = 100 nm) across an array of Si nanoantennas. (c)(d) Zoom-in of Figure 5d showing NS release, Brownian diffusion and transport from one illuminated nanoantenna to another.

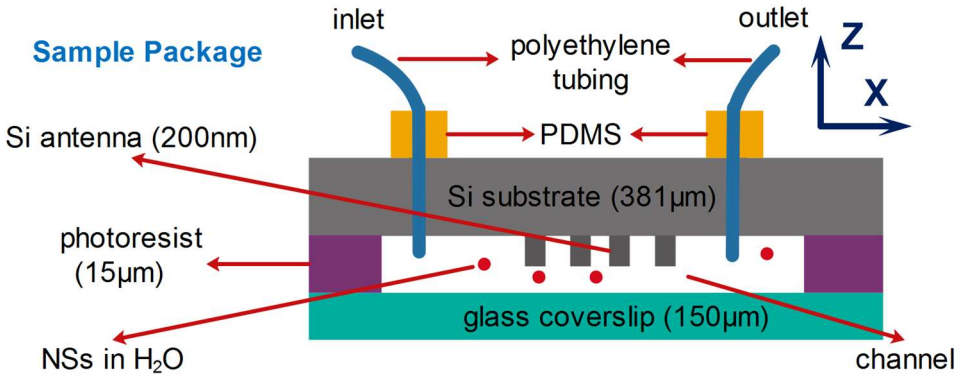

Figure S14 | Microfluidic chamber. Cross section of closed perfusion chamber, sealed with UV-cured optical adhesives.

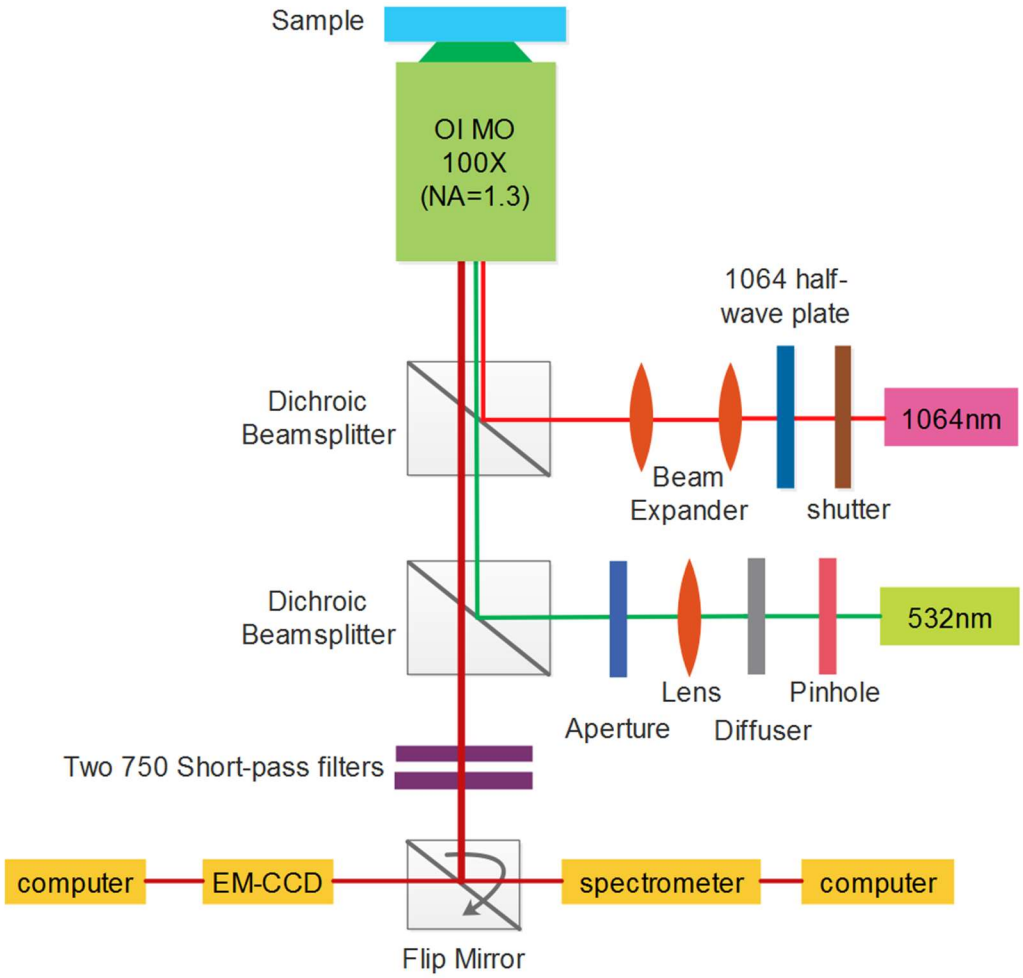

Figure S15 | Schematic diagram of experimental setup. The trapping is monitored by observing the NSs fluorescence. (OI MO = Oil Immersion Microscope Objective)

Movies

Movie 1. Optical trapping and release of a single 20 nm polystyrene nanosphere.

Movie 2. Optical trapping and release of two 20 nm polystyrene nanospheres.

Movie 3. Optical trapping and release of a single 100 nm polystyrene nanosphere.

Movie 4. Optical trapping and release of two 100 nm polystyrene nanospheres.

Movie 5. Optical trapping and release of three 100 nm polystyrene nanospheres.

Movie 6. Optical trapping and transport of a single 100 nm polystyrene nanosphere.

Movie 7. Optical trapping and transport of two 100 nm polystyrene nanospheres.

References

(1) Palik, E. D. *Handbook of Optical Constants of Solids*; Academic Press: New York, 2007.

(2) Johnson, P. B.; Christy, R. W. Optical constants of the noble metals. *Phys. Rev. B* **1972**, 6, 4370-4379.